PERGAMON

International Journal of Solids and Structures 40 (2003) 2249–2266

INTERNATIONAL JOURNAL OF SOLIDS and STRUCTURES

www.elsevier.com/locate/ijsolstr

# Biaxial flexural strength distribution of thin ceramic substrates with surface defects

Ming Cheng, Weinong Chen *, K.R. Sridhar

*Department of Aerospace and Mechanical Engineering, The University of Arizona, Tucson, AZ 85721-0119, USA*

Received 6 December 2001; received in revised form 8 January 2003

**Abstract**

The statistical models of the strength of thin ceramic substrates with surface defects under piston-on-3-ball loading conditions are formulated using Batdorf's statistical theory and Kirstein and Woolley's moment equations. These models possess the form of a Weibull distribution function, making it possible to process the piston-on-3-ball biaxial flexural strength data using a Weibull treatment. During this study, it was noted that the thickness of the specimen had no effect on the failure distribution. Therefore, it was deemed that a reasonable thickness of the specimen disk could be selected for the piston-on-3-ball test in the case where the thickness is so small that the deflection of the center of the specimen exceeds half of the thickness (this thickness would invalidate the strength evaluation equation specified in ASTM F 394-78). The strengths of seven different compositions of 8YSZ with dopants were tested using the piston-on-3-ball method. The results were then processed using the derived models. The failure distributions of the different thickness groups of 8YSZ specimens were similar, verifying that the thickness, indeed, has no effect on the failure distribution.


*Keywords:* Biaxial flexural strength; Ceramic substrate; Piston-on-3-ball; Weibull

## 1. Introduction

Biaxial flexural strength tests have been widely accepted for evaluating the mechanical properties of thin ceramic substrates. Many test configurations have been established, such as ring-on-ring, piston-on-ring, ball-on-ring, piston-on-3-ball, and ball-on-3-ball (Watchman et al., 1972). Although the ball-on-ring configuration was reported to be the ideal method among these loading configurations (Shetty et al., 1980; With and Wagemans, 1989) to determine materials properties, and a number of advanced hydraulic loading facilities were developed (Gorham and Rickerby, 1975; Shetty et al., 1983; Chao and Shetty, 1991), the piston-on-3-ball method was adopted by the American Society of Test and Materials as a standard test method (ASTM F 394-78, 1995) for thin ceramic substrates. In spite of the fact that the stress under the piston is practically nonuniform and difficult to model, this method has the advantages that three balls support the

* Corresponding author. Tel.: +1-520-621-6114; fax: +1-520-621-8191.
*E-mail address:* weinong@u.arizona.edu (W. Chen).

0020-7683/02/$ - see front matter © 2002 Elsevier Science Ltd. All rights reserved.
doi:10.1016/S0020-7683(03)00052-0

specimens, allowing the use of a slightly warped specimen, and no surface grinding or polishing is required, in contrast to the ring-supported techniques. It is possible, therefore, to analyze the effects of processing parameters on the surface of the specimen using the piston-on-3-ball method. This method is thus effective in determining the relative strength of specimens where precise knowledge of the fracture stress is not necessary, such as the situations of quality control in plants and laboratory benchmarking tests in new material development.

Ceramic strength data are typically scattered over a wide range (compared to metal materials) and must be processed statistically. The Weibull distribution has been widely used in processing ceramic strength data in order to account for the wide scattering of such data. Weibull's strength theory of brittle materials is a pure statistical model. Previous research activities have mostly been focused on the application of the Weibull distribution to interpret strength data on the basis of uniaxial loading conditions. There was no existing mechanism-based analytical method for deducing the statistics of fracture under more general stress states until Batdorf's theory was published (Batdorf and Crose, 1974; Batdorf and Heinisch, 1978; Batdorf and Chang, 1979; Batdorf and Sines, 1980). Physical models still need to be developed to properly process the strength results obtained from biaxial stress loading tests.

A physics-based statistical model must consider two key factors that dominate brittle fracture under multi-axial loading conditions—the statistical nature of fracture and the multi-axial stress state that causes the fracture. The statistics of fracture under multi-axial stresses have been studied by Batdorf and his co-workers (Batdorf and Crose, 1974; Batdorf and Heinisch, 1978; Batdorf and Chang, 1979; Batdorf and Sines, 1980) and by Evans (1978). Although Batdorf and his co-workers and Evans proposed two different theories for multi-axial fractures, Chao and Shetty (1990) proved that the theories were equivalent if the same fracture criterion and flaw size distribution were used. Furthermore, they developed failure probability formulations based on Batdorf's theory for the test configurations of uniaxial tension, three- and four-point bending, and the ring-on-ring method (Chao and Shetty, 1991). Although the intrinsic nature of multi-axial stress states near the crack tips was not accounted for, these models were an important advancement in the interpretation of the statistical nature of multi-axial brittle fractures.

The Weibull treatment of strength data is usually employed in the ASTM standard test methods for uniaxial flexural strength of ceramic materials (ASTM C 1161-94, 1995; ASTM C 1211-92, 1995; ASTM C 1273-95a, 1995). However, there is no suitable model to interpret the results obtained by the ASTM standard test method for the biaxial flexural strength of ceramic substrates (piston-on-3-ball method), perhaps due to the lack of statistical models for this loading configuration. Although rigorous theoretical proof does not exist, some researchers have heuristically fitted their piston-on-3-ball strength data with the standard Weibull distribution function and used the Weibull modulus to compare the results obtained from three- and four-point bending tests that had uniaxial stress states at the specimen surfaces (Cattell et al., 2001). This use points out the need for an analytical statistical model for the piston-on-3-ball test configuration so the statistics of the test data can be interpreted, analyzed, and applied properly.

In this paper, specific statistical models for the piston-on-3-ball method are formulated by following the same procedure used by Chao and Shetty (1991), who developed statistical models for many other loading conditions, such as uniaxial, three- and four-point bending, and ring-on-ring loading configurations. The formulations are based on studies by two research groups: Batdorf and Crose (1974), who developed a general statistical theory for the fracture of a brittle structure subjected to nonuniform multi-axial stresses, and Kirstein and Woolley (1967), who developed equations that could be used for evaluating the moments in the piston-on-3-ball loading configuration, which can then be used to derive formulations for evaluating the stresses in the tensile surface. The stresses in the tensile surface are the key to the application of Batdorf's theory. The resultant specific statistical models for biaxial brittle fracture are applied to the strength analysis of 8-mol% yttria stabilized zirconia (8YSZ) thin substrates under piston-on-3-ball loading conditions. Since the specimens are tested at as-fired conditions, the fractures are considered to be initiated at defects in the tensile surface where the most significant tensile stresses occur. By SEM examination of the

fracture surfaces of the tested specimen, Selçuk and Atkinson (2000) revealed that the fracture of 8YSZ thin substrates under ring-on-ring loading conditions was also initiated at defects in the tensile surface. Here, only statistical models with fractures caused by surface flaws are formulated. Multi-axial fractures initiated at volume flaws can be modeled in the same manner.

## 2. Theories

Batdorf's theory for multi-axial stress state loading conditions requires a fracture criterion for determining the solid angle, which is defined as the angle in the principal stress space enclosing all the normals to crack planes so that an effective stress, which is based on the stress state and crack orientation, will satisfy the fracture criterion. In this section, the stress distribution on the tensile surface will be introduced first. Then the stress distribution will be applied to a specific fracture criterion to obtain the solid angle.

### 2.1. Stress evaluation

Bassali (1957) formulated the general solution to the problem of flexure of a thin circular elastic plate supported at an arbitrary number of points, which may be located anywhere within the plate periphery, and loaded perpendicular to the plate over a circular area lying anywhere within the boundary of the plate. Kirstein and Woolley (1967) specified Bassali's theory to provide solutions to the problem of symmetrical bending of thin circular elastic plates on equally spaced point supports. With these solutions, the equations for evaluating the stress state on the tensile surface of the specimen plate can be formulated. The contribution of direct shear forces to the stress is ignored, which is justified by the fact that the thickness of the plate is much less than the in-plane dimensions, such that the plate can be considered as a slender structure. Some of the parameters are given in Fig. 1, and a schematic of the specimen plate and loading/supporting conditions is shown in Fig. 2.

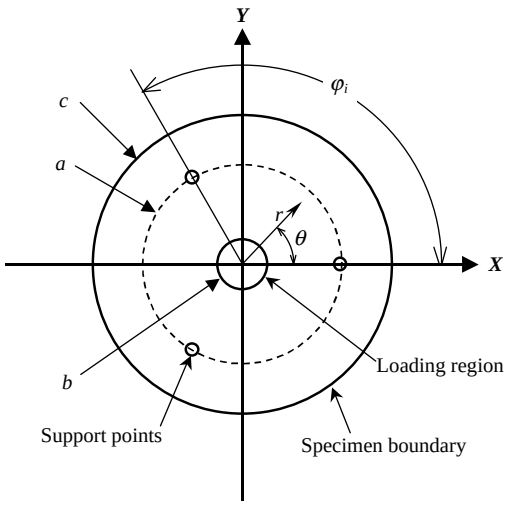


Fig. 1. Parameters in the piston-on-3-ball configuration: $a$ = radius of the concentric support circle, $b$ = radius of the loaded area (radius of the piston), $c$ = radius of the plate specimen, and $\varphi_i = \theta - 2\pi i/3$ $(i = 1, 2, 3)$.

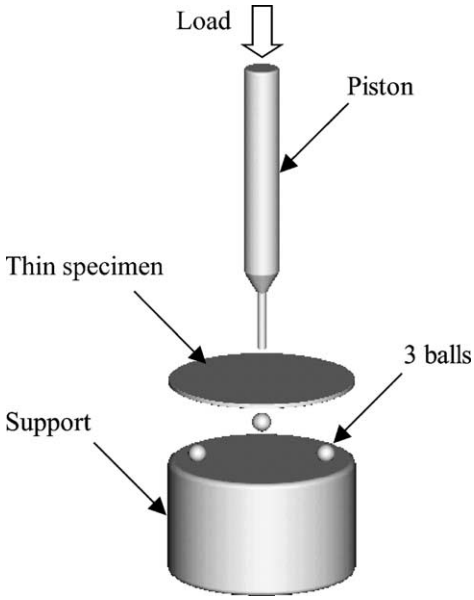


Fig. 2. Piston-on-3-ball experimental configuration.

The in-plane stresses are conveniently expressed in a polar coordinate system with normalized radius $\rho$ ($0 \leqslant \rho \leqslant 1$), which starts from the center of the specimen surface, and polar angle $\theta$ which starts from the positive $X$ axis that passes through one of the supports (Fig. 1). By using Kirstein and Woolley's equations for bending and twisting moments, the in-plane stresses on the tensile surface due to the out-of-plane load $P$ can be derived as follows:

$$\sigma_{rr} = P\bar{f}_{rr}(\rho,\theta)\frac{6}{h^2} \tag{1}$$

$$\sigma_{\theta\theta} = P\bar{f}_{\theta\theta}(\rho,\theta)\frac{6}{h^2} \tag{2}$$

and

$$\sigma_{r\theta} = P\bar{f}_{r\theta}(\rho,\theta)\frac{6}{h^2} \tag{3}$$

where $h$ is the thickness of the plate, $\rho$ is the normalized polar radius coordinate ($r/c$), and $\bar{f}_{rr}(\rho,\theta)$, $\bar{f}_{\theta\theta}(\rho,\theta)$, and $\bar{f}_{r\theta}(\rho,\theta)$ are stress distribution functions that are independent of loading levels and plate thickness and are expressed as follows:

$$\bar{f}_{rr}(\rho,\theta) = -\frac{1+v}{24\pi\kappa}\Psi + \frac{1-v}{48\pi\kappa\rho^2}\Theta$$

$$\bar{f}_{\theta\theta}(\rho,\theta) = -\frac{1+v}{24\pi\kappa}\Psi - \frac{1-v}{48\pi\kappa\rho^2}\Theta$$

$$\bar{f}_{r\theta}(\rho,\theta) = \frac{1-v}{24\pi\kappa\rho^2}\Phi$$

where $\kappa$ is defined as $(3+v)/(v-1)$, $v$ is Poisson's ratio, and $\Psi$ is defined as

$$\Psi = \overline{\Psi} + \begin{cases} 6\kappa \ln q + \dfrac{3\kappa\rho^2}{q^2} - 3\kappa, & \rho \leqslant q \\ 6\kappa \ln \rho, & \rho > q \end{cases}$$

with the first term defined as

$$\overline{\Psi} = \sum_{i=1}^{3} \overline{\Psi}_i - \frac{6t^2\left(1+\dfrac{\kappa q^2}{2-t^2}\right)}{\kappa+1} + 3(1+t^2)$$

$$\overline{\Psi}_i = \ln(1 - 2\rho t\cos\varphi_i + \rho^2 t^2) - \kappa \ln(\rho^2 - 2\rho t\cos\varphi_i + t^2) - \frac{(1-t^2)(1-\rho^2 t^2)}{1 - 2\rho t\cos\varphi_i + \rho^2 t^2}$$

where $q$ is defined as $b/c$, and $t$ is defined as $a/c$. In addition, $\Theta$ is defined as

$$\Theta = \overline{\Theta} + \begin{cases} -\dfrac{3\kappa\rho^4}{q^2}, & \rho \leqslant q \\ -6\kappa\rho^2 + 3\kappa q^2, & \rho > q \end{cases}$$

with the first term defined as

$$\overline{\Theta} = \sum_{i=1}^{3} \overline{\Theta}_i + 3(\kappa-1)(\rho^2 - t^2)$$

$$\overline{\Theta}_i = (\kappa^2-1)\ln(1 - 2\rho t\cos\varphi_i + \rho^2 t^2) + \frac{(1-\rho^2 t^2)^2 - 2t^2(1-\rho^2)^2}{1 - 2\rho t\cos\varphi_i + \rho^2 t^2} - \frac{(1-\rho^2)(1-t^2)(1-\rho^2 t^2)^2}{(1 - 2\rho t\cos\varphi_i + \rho^2 t^2)^2} + \frac{\kappa(\rho^2 - t^2)^2}{\rho^2 - 2\rho t\cos\varphi_i + t^2}$$

$\Phi$ is defined as

$$\Phi = \sum_{i=1}^{3} \Phi_i$$

$$\Phi_i = \frac{\rho t\sin\varphi_i(\rho^2 - t^2)}{1 - 2\rho t\cos\varphi_i + \rho^2 t^2} - \frac{\rho t\sin\varphi_i(1-\rho^2)(1-t^2)(1-\rho^2 t^2)}{(1 - 2\rho t\cos\varphi_i + \rho^2 t^2)^2} - \frac{\kappa\rho t\sin\varphi_i(\rho^2 - t^2)}{\rho^2 - 2\rho t\cos\varphi_i + t^2} - (\kappa^2-1)\arctan\frac{\rho t\sin\varphi_i}{1 - \rho t\cos\varphi_i}$$

The stress distributions expressed by Eqs. (1)–(3) have a singular point at the center of the plate where $\rho$ is equal to zero. By further analysis of stresses at this point (Kirstein and Woolley, 1967), it was concluded that the tensile stresses reach their maximum values at the center of the surface,

$$\sigma_{rr} = \sigma_{\theta\theta} = \sigma_{\mathrm{b}} = P\bar{f}_{\mathrm{c}}\frac{6}{h^2} \tag{4}$$

and

$$\sigma_{r\theta} = 0 \tag{5}$$

where

$$\bar{f}_c = -\frac{(1+v)}{8\pi}\left[\frac{2t^2\left(1-\frac{q^2}{2t^2}\right)}{\kappa+1}+2\ln\frac{q}{t}-1\right]$$

As described by Eqs. (1)–(4), all the stresses are proportional to the piston load $P$ and inversely proportional to the square of the specimen thickness. However, each stress has its own distribution function, independent of loading level, as described by $\bar{f}_{rr}(\rho,\theta)$, $\bar{f}_{\theta\theta}(\rho,\theta)$, and $\bar{f}_{r\theta}(\rho,\theta)$. Therefore, the stress distributions can be normalized by the stresses at the center. The normalized stress distribution functions $f_{rr}(\rho,\theta)$, $f_{\theta\theta}(\rho,\theta)$, and $f_{r\theta}(\rho,\theta)$ are independent of the piston load and the thickness of the specimen. In terms of $f_{rr}(\rho,\theta)$, $f_{\theta\theta}(\rho,\theta)$, and $f_{r\theta}(\rho,\theta)$, the stress distributions in the tensile surface of the plate can be expressed as follows:

$$\sigma_{rr} = \sigma_b \frac{\bar{f}_{rr}(\rho,\theta)}{\bar{f}_c} = \sigma_b f_{rr}(\rho,\theta) \tag{6}$$

$$\sigma_{\theta\theta} = \sigma_b \frac{\bar{f}_{\theta\theta}(\rho,\theta)}{\bar{f}_c} = \sigma_b f_{\theta\theta}(\rho,\theta) \tag{7}$$

and

$$\sigma_{r\theta} = \sigma_b \frac{\bar{f}_{r\theta}(\rho,\theta)}{\bar{f}_c} = \sigma_b f_{r\theta}(\rho,\theta) \tag{8}$$

With the stress components $\sigma_{rr}$, $\sigma_{r\theta}$, and $\sigma_{\theta\theta}$ known, the principal stresses at any point $(\rho,\theta)$ on the tensile surface of the specimen can be calculated by

$$\sigma_r = \frac{\sigma_{rr}+\sigma_{\theta\theta}}{2} + \sqrt{\left(\frac{\sigma_{rr}-\sigma_{\theta\theta}}{2}\right)^2+\sigma_{r\theta}^2} = \sigma_b f_r(\rho,\theta) \tag{9}$$

and

$$\sigma_\theta = \frac{\sigma_{rr}+\sigma_{\theta\theta}}{2} - \sqrt{\left(\frac{\sigma_{rr}-\sigma_{\theta\theta}}{2}\right)^2+\sigma_{r\theta}^2} = \sigma_b f_\theta(\rho,\theta) \tag{10}$$

The stress state at an arbitrary point on the tensile surface serves as the base for developing a statistical model to describe the fracture strength of brittle materials using Batdorf's theory. In the following section, the equations given above for evaluating the stresses on the tensile surface will be used together with fracture criteria to develop statistical models for brittle fracture under piston-on-3-ball loading condition.

### 2.2. Statistical model

Batdorf and his co-workers developed a statistical theory for the fracture of brittle structures subjected to nonuniform multi-axial stress state (Batdorf and Crose, 1974; Batdorf and Heinisch, 1978; Batdorf and Chang, 1979; Batdorf and Sines, 1980). According to this theory, the cumulative probability distribution (failure probability), $P_f$, of fracture due to surface defects is given by

$$P_f = 1 - \exp\left[-\int_A\int_0^{\sigma_h}\frac{\Omega}{2\pi}\frac{dN(\sigma_{cr})}{d\sigma_{cr}}\,d\sigma_{cr}\,dA\right] \tag{11}$$

where $\sigma_{cr}$ is, according to Batdorf's definition, the remote critical normal stress that causes fracture when a uniform uniaxial stress is applied normal to the plane of a crack; $\sigma_h$ is the highest value that $\sigma_{cr}$ can achieve;

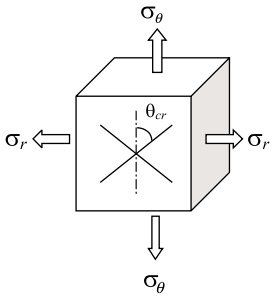


Fig. 3. Critical angle for randomly oriented surface cracks in a biaxial stress state.

$A$ is the tensile surface area; and $\Omega$ is the solid angle containing the normals to all orientations for which the component of the applied stress normal to the crack plane is larger than $\sigma_{cr}$. In the case of a biaxial stress state (Fig. 3),

$$\Omega = 4\theta_{cr} \tag{12}$$

where $\theta_{cr}$ is the largest angle of the orientation of the crack associated with the critical stress $\sigma_{cr}$. All the cracks associated with the critical stress $\sigma_{cr}$ with orientation angles less than $\theta_{cr}$ will lead to fracture. $N(\sigma_{cr})$ is the crack size distribution function on the tensile surface, which gives the density of cracks having a critical stress less than or equal to $\sigma_{cr}$. Batdorf and coworkers proposed to represent $N(\sigma_{cr})$ by a Taylor series. However, Chao and Shetty (1991) used a relatively simple form for the crack size distribution function

$$N(\sigma_{cr}) = \bar{k}\sigma_{cr}^{m} \tag{13}$$

where $\bar{k}$ and $m$ are the scale and shape parameters, respectively, in analogy to the Weibull parameters.

When Eq. (13) is used to describe the crack size distribution, the cumulative probability distribution has the form

$$P_f = 1 - \exp\left[ -\int_A \int_0^{\sigma_h} \frac{4\theta_{cr}}{2\pi} \bar{k} m \sigma_{cr}^{m-1} \, d\sigma_{cr} \, dA \right] = 1 - \exp\left( -\frac{2}{\pi} \bar{k} m \sigma_b^m I_B \right) \tag{14}$$

where the scale factor $I_B$ is evaluated by

$$I_B = c^2 \int_0^{2\pi} \int_0^1 \int_0^{\sigma_h/\sigma_b} \theta_{cr} \left( \frac{\sigma_{cr}}{\sigma_b} \right)^{m-1} d\left( \frac{\sigma_{cr}}{\sigma_b} \right) \rho \, d\rho \, d\theta \tag{15}$$

Since the crack extension initiates exclusively on the tensile free surface, the fractures under biaxial flexural stress conditions are considered to involve only mode I and mode II cracks. Chao and Shetty (1991) considered two failure criteria to determine the solid angle. The first one was the critical normal stress criterion, which considered failure to be determined solely by the mode I loading of a crack

$$K_I = K_{IC} \tag{16}$$

where $K_I$ is the mode I stress intensity factor and $K_{IC}$ is the mode I fracture toughness of the material. The second failure criterion was the noncoplanar strain release rate criterion

$$\left( \frac{K_I}{K_{IC}} \right) + \left( \frac{K_{II}}{CK_{IC}} \right)^2 = 1 \tag{17}$$

where $K_{II}$ is the mode II stress intensity factor and $C$ is a constant. This equation was originally suggested by Palaniswamy and Knauss (1978) using the shear-sensitivity parameter $C = \sqrt{2/3} \approx 0.82$. Singh and

Shetty (1989a) showed that $C$ took values in the range of 1–2 for polycrystalline ceramics under combined mode I and mode II loading conditions. The higher the value of $C$, the lower the shear sensitivity of the material.

If the crack on the tensile surface is assumed to be in the shape of a half penny, the mode I and mode II stress intensity factors for a half-penny surface crack subjected to general remote loading are as follows (Kassir and Sih, 1966; Sih, 1984):

$$K_{\mathrm{I}} = \frac{2M_{\mathrm{I}}\sigma_{\mathrm{N}}\sqrt{a}}{\sqrt{\pi}} \tag{18}$$

$$K_{\mathrm{II}} = \frac{4M_{\mathrm{II}}\tau\sqrt{a}}{\sqrt{\pi}(2-\nu)} \tag{19}$$

where $\sigma_{\mathrm{N}}$ and $\tau$ are normal and shear stresses, respectively, and $M_{\mathrm{I}}$ and $M_{\mathrm{II}}$ are free surface and stress gradient correction factors. Since $M_{\mathrm{I}}$ and $M_{\mathrm{II}}$ are approximately equal to each other (Smith and Sorensen, 1975; Newman and Raju, 1981), the two fracture criteria, Eqs. (16) and (17), become

$$\sigma_{\mathrm{N}} = \sigma_{\mathrm{cr}} \tag{20}$$

and

$$\frac{\sigma_{\mathrm{N}}}{\sigma_{\mathrm{cr}}} + \left[\frac{2\tau}{C(2-\nu)\sigma_{\mathrm{cr}}}\right]^2 = 1 \tag{21}$$

For a general biaxial stress state at an arbitrary location on the tensile surface, the normal stress $\sigma_{\mathrm{N}}$ and shear stress $\tau$ can be evaluated as

$$\sigma_{\mathrm{N}} = \frac{\sigma_r + \sigma_\theta}{2} - \frac{\sigma_r - \sigma_\theta}{2}\cos(2\theta) \tag{22}$$

and

$$\tau = -\frac{\sigma_r - \sigma_\theta}{2}\sin(2\theta) \tag{23}$$

By substituting Eqs. (22) and (23) into the critical normal stress criterion, Eq. (20), and using Eqs. (9) and (10), $\sigma_{\mathrm{cr}}/\sigma_{\mathrm{b}}$ is found to be

$$\frac{\sigma_{\mathrm{cr}}}{\sigma_{\mathrm{b}}} = \frac{(f_r + f_\theta)}{2} - \frac{(f_r - f_\theta)}{2}\cos(2\theta_{\mathrm{cr}}) = f_{\mathrm{N}}(\rho, \theta, \theta_{\mathrm{cr}}) \tag{24}$$

Furthermore, by applying differentiation to Eq. (24), we obtain

$$\mathrm{d}\left(\frac{\sigma_{\mathrm{cr}}}{\sigma_{\mathrm{b}}}\right) = (f_r - f_\theta)\sin(2\theta_{\mathrm{cr}})\,\mathrm{d}\theta_{\mathrm{cr}} \tag{25}$$

Therefore, by substituting Eqs. (24) and (25) into Eq. (15), the scale factor $I_{\mathrm{B}}$ can be obtained as

$$I_{\mathrm{B}} = c^2 \int_0^{2\pi}\int_0^1\int_0^{\pi/2} \theta_{\mathrm{cr}}[f_{\mathrm{N}}H(f_{\mathrm{N}})]^{m-1}(f_r - f_\theta)\sin(2\theta_{\mathrm{cr}})\rho\,\mathrm{d}\theta_{\mathrm{cr}}\,\mathrm{d}\rho\,\mathrm{d}\theta \tag{26}$$

where $H(f_{\mathrm{N}})$ is the Heaviside step function. The reason for employing the Heaviside step function is to avoid counting the contribution from the compressive normal stresses, since the compressive stresses normal to a crack will not cause fracture in brittle materials. An analysis using the finite element method or Bassali's theory shows that the maximum principle stresses are compressive in the vicinity of the three support balls on the tensile surface. Therefore, fracture cannot occur there.

The noncoplanar strain release rate criterion takes both the mode I and mode II loadings into consideration, which is more proper for shear-sensitive materials. The scale factor for this criterion can be obtained by substituting Eqs. (22) and (23) into Eq. (21) and using Eqs. (9) and (10). Therefore, $\sigma_{cr}/\sigma_b$ and its differentiation are found to be

$$\frac{\sigma_{cr}}{\sigma_b} = F(\rho,\theta,\theta_{cr}) = \frac{f_N}{2} + \frac{\sqrt{C^2(2-\nu)^2 f_N^2 + 4(f_r - f_\theta)^2 \sin^2(2\theta_{cr})}}{2C(2-\nu)} \tag{27}$$

and

$$\begin{aligned} d\left(\frac{\sigma_{cr}}{\sigma_b}\right) &= \frac{\partial F(\rho,\theta,\theta_{cr})}{\partial\theta_{cr}}\, d\theta_{cr} \\ &= \frac{8(f_r - f_\theta)^2 \sin(2\theta_{cr})\cos(2\theta_{cr}) + 2\left(\frac{\sigma_{cr}}{\sigma_b}\right) C^2(2-\nu)^2 (f_r - f_\theta)\sin(2\theta_{cr})}{C^2(2-\nu)^2\left[4\left(\frac{\sigma_{cr}}{\sigma_b}\right) - (f_r + f_\theta) + (f_r - f_\theta)\cos(2\theta_{cr})\right]}\, d\theta_{cr} \end{aligned} \tag{28}$$

In this case, the scale factor $I_B$ is obtained as

$$I_B = c^2 \int_0^{2\pi}\int_0^1\int_0^{\pi/2} \theta_{cr}[FH(f_N)]^{m-1} \frac{\partial F}{\partial\theta_{cr}} \rho\, d\theta_{cr}\, d\rho\, d\theta \tag{29}$$

Therefore, it has been proven by these formulae that the failure distribution of a thin ceramic substrate with piston-on-3-ball loading conditions is in the form of a Weibull distribution function, as indicated by Eq. (14). The scale factor $I_B$ is an important parameter in the probability distribution. Once the flaw size distribution function in the tensile surface, $N(\sigma_{cr})$, is determined, the smaller the scale factor $I_B$, the smaller the failure probability at a certain strength level. Therefore, the scale factor $I_B$ can be used as an indicator of reliability. The studies of the sensitivity of the scale factor $I_B$ to Poisson's ratio are shown in Figs. 4 and 5, with a specimen geometry ($a = 12.7$ mm, $b = 0.8$ mm, and $c = 15.9$ mm) recommended by ASTM F 394-78 and a shape parameter $m = 7.1$. Fig. 4 shows that the noncoplanar strain energy release rate criterion is safer to use than the critical normal stress criterion if the shear-sensitivity parameter $C$ is chosen to be 0.82

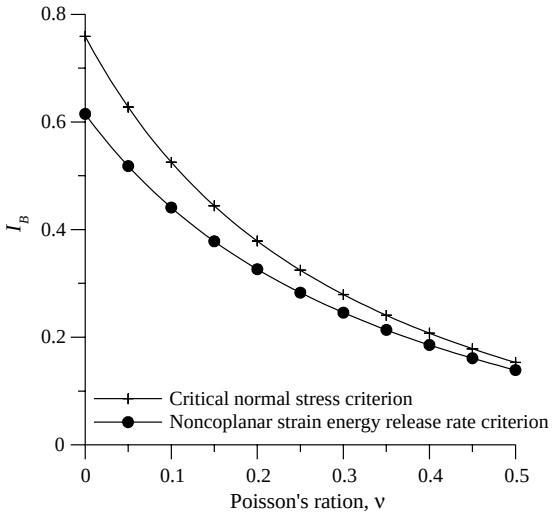


Fig. 4. Variation of the scale factor $I_B$ for different fracture criteria ($C = 0.82$ for the noncoplanar strain energy release rate criterion).

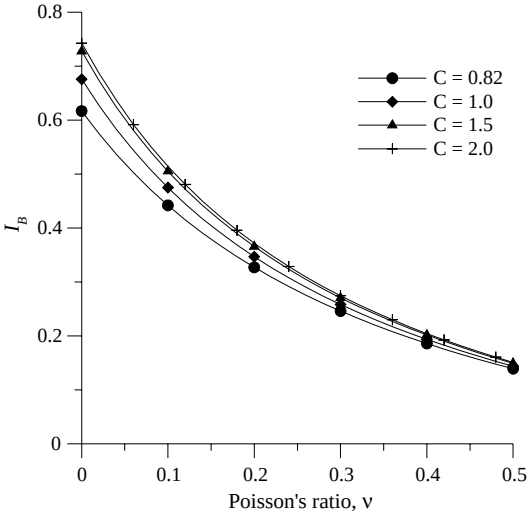


Fig. 5. Variation of scale factor $I_B$ with the noncoplanar strain energy release rate fracture criteria with different values of the shear-sensitivity parameter $C$.

as recommended by Palaniswamy and Knauss (1978), especially for brittle materials with small Poisson's ratios. This is because the noncoplanar strain energy release rate criterion takes mode II loading into account, in addition to the mode I loading.

Fig. 5 shows that the scale factor $I_B$ is dependent on the value of the shear-sensitivity parameter $C$. With $C$ increasing from 0.82 to 2, the scale factor, $I_B$, increases. When checking the numerical values of these data, it was observed that the critical normal stress criterion is equivalent to the noncoplanar strain energy release rate criterion provided the value of $C$ is 2, which is the upper limit proposed by Shetty and co-workers (Shetty, 1987; Singh and Shetty, 1989a,b).

### 2.3. Discussion

With the cumulative probability distribution functions derived above, it has been proven that the Weibull distribution may also be used to describe the biaxial flexural strength of ceramic thin substrates under piston-on-3-ball loading conditions. As in the cases of three- and four-point bending experiments (Wachtman, 1996), the strength data can be fitted to a Weibull distribution function to obtain the Weibull parameters. In the case of piston-on-3-ball experiments, the Weibull shape parameter, $m$, and crack density scale parameter, $\bar{k}$, can be identified from a group of piston-on-3-ball test data. Eq. (13) shows that these two parameters characterize the surface flaw population of the test material with associated specific material processing parameters. Therefore, they provide a method to estimate the fracture distribution of the same material with the same processing parameters, but with different geometry and loading conditions. For example, we can estimate the strength of a bar with three- or four-point bending conditions using the cumulative probability distribution formulations derived by Chao and Shetty (1991). Furthermore, with the stress distribution of a structure analyzed using a finite element program, the cumulative probability distribution can be numerically calculated following the same procedure as that applied to derive the cumulative probability distributions in this paper.

An important observation was made from the derivation of the cumulative probability distribution formulae [see Eqs. (6)–(8)]. The thickness, $h$, of the specimen does not contribute anything to the final

results as it is cancelled in the process of derivation. This is because we assumed that the fracture resulted from the surface defects. Changing the thickness does not change the surface crack distribution. Therefore, it provides us with a flexible way to prepare specimens. It is known from fracture mechanics that the geometry of the specimen has strong effects on the strength (Hoshide et al., 1998). Thus, in practice, the sizes of the specimens must be designed as close as possible to the sizes of the real structures. Sometimes, the actual structure must be designed to be very thin (<0.5 mm), making its use as a specimen for piston-on-3-ball experiments impossible since such experiments require that the deflection of the specimen must be less than half of the thickness of the specimen to obtain valid data. When surface defects are the main fracture initiators, we can use test data from a group of reasonably thicker specimens to represent the fracture distribution of the thin structure.

It should be pointed out that the employment of two failure criteria—the critical normal stress criterion and the noncoplanar strain release rate criterion—to determine the solid angle is not sufficient to cover all possible failure mechanisms. The critical normal stress criterion considers only the failure caused by mode I loading on a crack. Although the noncoplanar strain release rate criterion takes the mode II loading into account, it dismisses the effect of interaction between mode I and mode II loadings. To take the interactions into account, a strain energy density criterion (Sih, 1974; Sih and Barthelemy, 1980) may be employed. In the plane problem, a strain energy density factor is defined as

$$S = a_{11}K_{\mathrm{I}}^2 + 2a_{12}K_{\mathrm{I}}K_{\mathrm{II}} + a_{22}K_{\mathrm{II}}^2 \tag{30}$$

where $a_{ij}$ $(i,j = 1,2)$ are

$$a_{11} = \frac{1}{16G}(3 - 4v - \cos\theta)(1 + \cos\theta)$$
$$a_{12} = \frac{1}{16G}2\sin\theta[\cos\theta - (1 - 2v)]$$
$$a_{22} = \frac{1}{16G}[4(1 - v)(1 - \cos\theta) + (1 + \cos\theta)(3\cos\theta - 1)]$$

with $G$ being the shear modulus of elasticity.

The strain energy density criterion states that (1) the direction of crack propagation coincides with the location of minimum strain energy density factor, $S_{\min}$ and (2) the crack extends when the minimum strain energy density factor reaches a critical value $S_{\mathrm{C}}$. The necessary and sufficient conditions for $S$ to be minimum are

$$\frac{\partial S}{\partial \theta} = 0 \tag{31}$$

and

$$\frac{\partial^2 S}{\partial \theta^2} > 0 \quad \text{for } \theta = \theta_0 \tag{32}$$

with $\theta_0$ corresponding to the direction of crack initiation, i.e., $S = S_{\min}$ for $\theta = \theta_0$. The critical value of $S_{\mathrm{C}}$ was given by Sih (1974) as

$$S_{\mathrm{C}} = \frac{(1 + v)(1 - 2v)K_{\mathrm{IC}}^2}{2\pi E} \tag{33}$$

The employment of this strain energy density criterion in the determination the solid angle results in the same form of distribution function—Weibull distribution. The difference is in the formulation for the scale factor $I_{\mathrm{B}}$. It is more general to use this strain energy density criterion to predict the strength distribution. However, the focus of this paper is to identify the form of strength distribution. $I_{\mathrm{B}}$ is part of a parameter

determined from experimental data, leaving the exact form of $I_B$ noncritical. Therefore, similar to the approach used by Chao and Shetty (1991), only simpler forms of failure criteria are employed here.

## 3. Experiments

### 3.1. Specimen preparation

The specimens were made from TZ-8YSZ powder (TOSOH USA, Inc., Atlanta, GA). The powder was mixed with dopants and was then processed into a slurry with dispersant, binder, and plasticizer, and the slurry was tape-cast. Then, the specimens were laser-cut out of green sheets and sintered at 1450 °C for 3 h. The surface roughness of as-fired specimens is between 20 and 30 μm as observed with a Zeiss IM 35 inverted microscope.

The geometry of the specimen is the one recommended by ASTM F 394-78: 32 mm in diameter and 0.76 mm in thickness. The specimen compositions studied in this research are listed in Table 1. In order to integrate this study with the study of physical properties, such as electrical conductivity from another research group (see Brach, 2000), the specimens prepared for this study are exactly the same as those specimens used for the study of physical properties. An X-ray diffraction (XRD) analysis performed on the materials revealed that only the cubic phase was present in all these specimens (Brach, 2000).

Table 1
Composition of specimens

| Composition | Alias |
|---|---|
| Pure 8YSZ | 8YSZ |
| 1 mol% $Al_2O_3$-doped 8YSZ | 1A |
| 2 mol% $Al_2O_3$-doped 8YSZ | 2A |
| 3 mol% $Al_2O_3$-doped 8YSZ | 3A |
| 10 wt% 3YSZ-doped 8YSZ | 1Y |
| 20 wt% 3YSZ-doped 8YSZ | 2Y |
| 30 wt% 3YSZ-doped 8YSZ | 3Y |

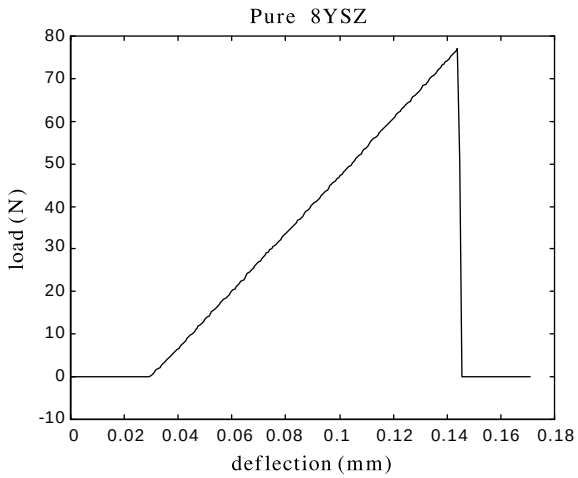


Fig. 6. A typical loading trace of the piston-on-3-ball experiment.

The surface condition of the specimens was made as close as possible to that to be used in service since the intention is to obtain realistic strength data for design. Therefore, the specimens used in this research had as-fired surface finishes. At this surface condition, the test results included all the factors that had effects on the biaxial flexural strength, such as material compositions and processing parameters, in addition to surface flaws.

### 3.2. Experimental procedure

In the piston-on-3-ball experimental method, a thin ceramic substrate is placed on three balls sitting 120° apart on a 25.4-mm-diameter circle (ASTM F 394-78, 1995). A piston pushes on the center of the circle from the other side of the ceramic sheet, thus producing a biaxial flexural loading condition, as shown in

Table 2
Biaxial flexural strength data (MPa) from experiments

| 8YSZ ($h = 0.76$ mm) | 8YSZ ($h = 0.41$ mm) | 1A | 2A | 3A | 1Y | 2Y | 3Y |
|---|---|---|---|---|---|---|---|
| 348.5 | 375.2 | 353.2 | 317.8 | 333.9 | 301.8 | 321.1 | 267.4 |
| 355.7 | 360.1 | 344.1 | 318.9 | 336.6 | 182.7 | 339.3 | 357.5 |
| 285.8 | 469.8 | 397.1 | 260.7 | 254.0 | 245.3 | 335.2 | 362.1 |
| 306.6 | 344.0 | 336.1 | 285.7 | 402.6 | 326.1 | 292.0 | 284.6 |
| 280.1 | 387.4 | 219.4 | 299.6 | 320.8 | 307.4 | 267.8 | 351.6 |
| 296.3 | 318.2 | 268.4 | 276.7 | 349.9 | 250.9 | 368.2 | 406.0 |
| 256.7 | 451.0 | 382.2 | 249.5 | | 251.8 | 375.3 | 324.6 |
| 346.4 | 327.3 | 313.5 | 301.9 | | 233.2 | 262.0 | 330.6 |
| 335.4 | 336.5 | 290.2 | 309.0 | | 245.8 | 346.0 | 411.2 |
| 333.3 | 236.0 | 330.1 | 349.7 | | 212.1 | 314.3 | 330.4 |
| 330.3 | 387.5 | 306.0 | 290.8 | | 257.3 | 301.0 | |
| 337.1 | 248.3 | 296.9 | 208.0 | | 308.7 | 245.1 | |
| 273.5 | 273.4 | 346.9 | 243.6 | | 232.9 | 306.7 | |
| 302.7 | 437.6 | 271.9 | 230.9 | | 194.9 | 277.4 | |
| 321.2 | | 286.7 | 210.2 | | 290.4 | 309.9 | |
| 355.0 | | 357.7 | | | 288.8 | | |
| 249.2 | | 378.2 | | | 271.3 | | |
| 283.9 | | | | | 292.3 | | |
| 337.5 | | | | | 293.6 | | |
| 303.9 | | | | | 185.3 | | |
| 382.6 | | | | | 301.3 | | |
| 381.2 | | | | | 302.7 | | |
| 280.3 | | | | | 267.9 | | |
| 356.2 | | | | | 319.2 | | |
| 179.6 | | | | | 284.6 | | |
| 363.5 | | | | | 265.0 | | |
| 393.2 | | | | | 271.5 | | |
| 339.1 | | | | | 95.4 | | |
| 274.1 | | | | | 159.9 | | |
| 297.4 | | | | | 172.9 | | |
| 388.9 | | | | | 367.6 | | |
| 218.2 | | | | | 263.8 | | |
| 210.9 | | | | | | | |
| 275.3 | | | | | | | |
| 299.4 | | | | | | | |

Fig. 2. The experiments were performed using a hydraulically driven material testing system (MTS 810) with a piston moving speed of less than 1.27 μm/s.

The experiments were performed at room temperature. The outputs of piston loading forces and specimen central deflection signals from the MTS 810 controller were recorded simultaneously using a National Instrument PCI-MIO-16XE-50 multifunction DAQ board that was installed in a personal computer. A data-acquisition control program was developed using LabVIEW 6*i*. Then, MATLAB 5.1 was used to process the original data. The statistics toolbox of MATLAB was used to do the Weibull analysis.

### *3.3. Experimental results*

A typical loading trace is shown in Fig. 6, which shows that the load increases linearly with deflection until failure, indicating a brittle failure at the peak load. The linearity of load with deflection is consistent with the analytical results derived by Kirstein et al. (1966).

The strength data were evaluated by the peak load using the equation for the stress at the center of the tensile surface, Eq. (4). Table 2 lists the strength data obtained from the piston-on-3-ball experiments.

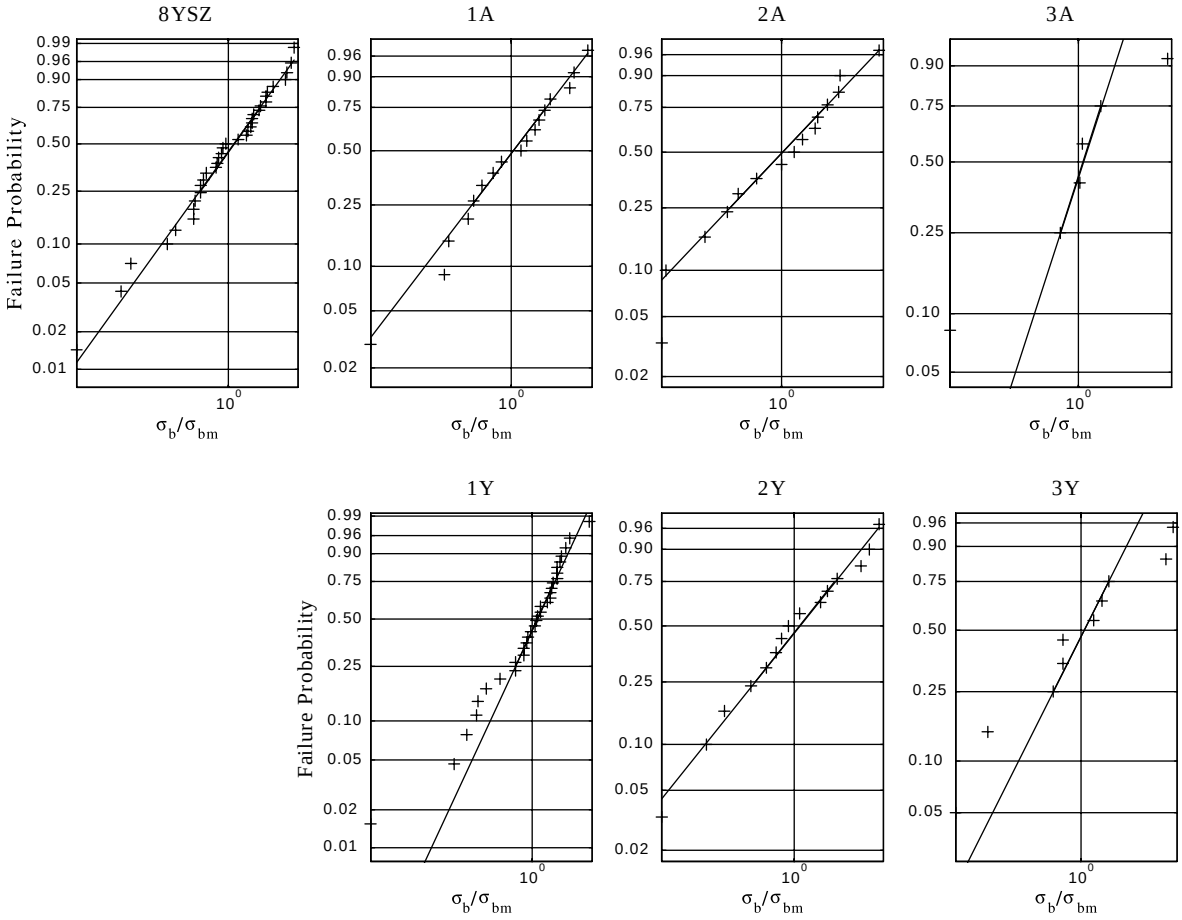


Fig. 7. Weibull probability plots of the biaxial flexural strengths from the piston-on-3-ball experiments.

Then, the data were fitted to the Weibull cumulative probability distribution function using the method of maximum likelihood (Jayatilaka, 1979),

$$P_f = 1 - \exp\left[-\alpha\left(\frac{\sigma_b}{\sigma_{bm}}\right)^m\right] \tag{34}$$

where $\alpha$ is a scale factor, $\sigma_b$ is the fracture stress, and $\sigma_{bm}$ is the mean of the fracture stress data. Then, the scale factor of the crack size distribution function [see Eq. (13)] is

$$\bar{k} = \frac{\pi}{2}\frac{1}{mI_B}\frac{\alpha}{\sigma_{bm}^m} \tag{35}$$

The data are shown as linearized Weibull plots in Fig. 7, and the associated Weibull parameters are listed in Table 3.

In order to verify that the thickness of the specimen does not contribute to the final cumulative probability distribution form, another group of 8YSZ specimens with different thickness was tested. The results are shown in Fig. 8 and listed in Table 4. The 95% confidence intervals of the Weibull parameters from

Table 3
Weibull parameters fitted from experimental results and biaxial flexural strengths

| Ceramic alias | Weibull parameters | | Strength (MPa) | |
|---|---|---|---|---|
| | $m$ | $\alpha$ | Mean | S.D. |
| 8YSZ | 7.44 (5.24, 9.65)[a] | 0.62 (0.40, 0.84) | 310.8 | 51.1 |
| 1A | 8.36 (4.51, 12.21) | 0.61 (0.31, 0.92) | 322.3 | 46.9 |
| 2A | 7.93 (4.30, 11.56) | 0.62 (0.30, 0.93) | 276.9 | 41.9 |
| 3A | 8.69 (2.13, 15.25) | 0.62 (0.14, 1.10) | 333.0 | 48.0 |
| 1Y | 5.68 (4.37, 7.00) | 0.64 (0.40, 0.87) | 257.6 | 56.5 |
| 2Y | 10.04 (4.48, 15.60) | 0.61 (0.29, 0.92) | 317.4 | 37.7 |
| 3Y | 8.81 (2.69, 14.92) | 0.62 (0.24, 1.00) | 342.6 | 46.0 |

[a] Inside the brackets is the 95% confidence interval.

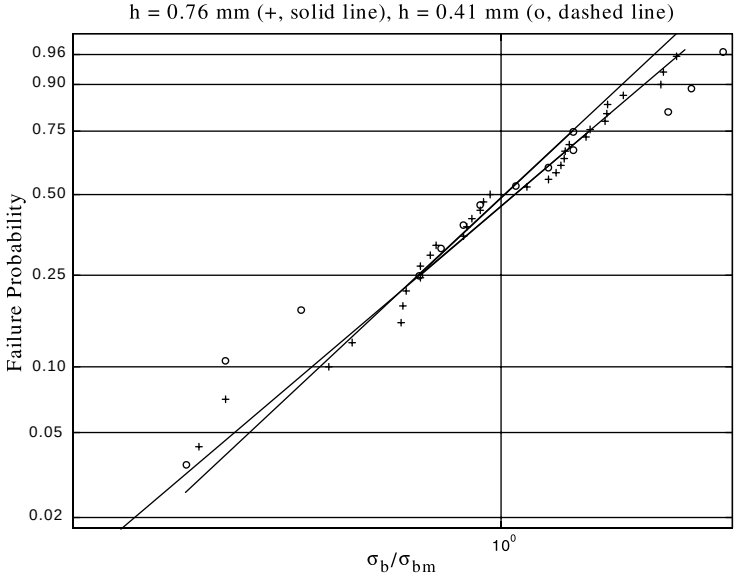


Fig. 8. Weibull probability plots for 8YSZ specimens with different thickness.

Table 4
Weibull parameters and biaxial flexural strength for 8YSZ with different specimen thickness

| Thickness (mm) | Weibull Parameters | | Strength (MPa) | |
|---|---|---|---|---|
| | $m$ | $\alpha$ | Mean | S.D. |
| 0.76 | 7.44 (5.24, 9.65)[a] | 0.62 (0.40, 0.84) | 310.8 | 51.1 |
| 0.41 | 5.83 (2.62, 9.04) | 0.64 (0.30, 0.98) | 342.6 | 46.0 |

[a] Inside the brackets is the 95% confidence interval.

these two group tests overlap and their mean strengths are approximately the same. These test results verify the validity of the new model for biaxial flexural strength under piston-on-3-ball loading conditions developed in this study.

## 4. Conclusions

Failure probability distribution function formulae for piston-on-3-ball loading conditions have been derived following Chao and Shetty's (1991) procedure for surface defects and using Batdorf's theory for biaxial flexural bending statistical model (Batdorf and Crose, 1974; Batdorf and Heinisch, 1978; Batdorf and Chang, 1979; Batdorf and Sines, 1980), and Bassali's (1957) theory for the evaluation of biaxial flexural bending stresses. The final formulae are in a form of the Weibull cumulative probability distribution function. Therefore, the experimental data from piston-on-3-ball tests can be processed with the Weibull treatment. The Weibull parameters are proven to be the characteristics of the population of surface defects. Therefore, these Weibull parameters can be used to predict the failure behavior of the tested material under other loading conditions.

Seven different compositions of 8YSZ with dopants were tested using the piston-on-3-ball method. The experimental results were processed using the Weibull treatment. The experimental data of 8YSZ with different thickness verify the fact that the thickness of the specimen does not have an effect on the failure probability distribution, which is derived from the statistical models. This fact indicates that the fracture of the 8YSZ substrates is indeed a result of surface defects.

## Acknowledgement

This research was supported by NASA through a grant (NAG 8-1469#4) to The University of Arizona.

## References

ASTM C 1161-94, 1995. Standard test method for flexural strength of advanced ceramics at ambient temperature. American Society of Testing and Materials Annual Book of Standards, ASTM, West Conshohocken, PA, vol. 15.01, pp. 304–310.

ASTM C 1211-92, 1995. Standard test method for flexural strength of advanced ceramics at elevated temperatures. American Society of Testing and Materials Annual Book of Standards, ASTM, West Conshohocken, PA, vol. 15.01, pp. 337–346.

ASTM C 1273-95a, 1995. Standard test method for tensile strength of monolithic advanced ceramics at ambient temperatures. American Society of Testing and Materials Annual Book of Standards, ASTM, West Conshohocken, PA, vol. 15.01, pp. 383–400.

ASTM F 394-78, 1995. Standard test method for biaxial flexural strength (modulus of rupture) of ceramic substrates. American Society of Testing and Materials Annual Book of Standards, ASTM, West Conshohocken, PA, vol. 15.01, pp. 469–473.

Bassali, W.A., 1957. The transverse flexure of thin elastic plates supported at several points. Proceedings of the Cambridge Philosophical Society 53, 728–743.

Batdorf, S.B., Chang, D.J., 1979. On the relation between the fracture statistical of volume distributed and surface-distributed cracks. International Journal of Fracture 15, 191–199.

Batdorf, S.B., Crose, J.G., 1974. A statistical theory for the fracture of brittle structures subjected to nonuniform polyaxial stresses. Journal of the American Ceramic Society 41, 459–465.

Batdorf, S.B., Heinisch Jr., H.L., 1978. Weakest link theory reformulated for arbitrary fracture criterion. Journal of the American Ceramic Society 61, 355–358.

Batdorf, S.B., Sines, G., 1980. Combining data for improved Weibull parameter estimation. Journal of the American Ceramic Society 63, 214–218.

Brach, S., 2000. Optimization of electrolyte material for use in solid oxide electrolysis cells. Master's thesis, The University of Arizona, Tucson.

Cattell, M.J., Chadwick, T.C., Knowles, J.C., Clarke, R.L., Lynch, E., 2001. Flexural strength optimisation of a leucite reinforced glass ceramic. Dental Materials 17, 21–33.

Chao, L.Y., Shetty, D.K., 1990. Equivalence of physically based statistical fracture theories for reliability analysis of structural ceramics in multiaxial loading. Journal of the American Ceramic Society 73, 1917–1921.

Chao, L.Y., Shetty, D.K., 1991. Reliability analysis of structural ceramics subjected to biaxial flexure. Journal of the American Ceramic Society 74, 333–344.

Evans, A.G., 1978. A general approach for the statistical analysis of multiaxial fracture. Journal of the American Ceramic Society 61, 302–308.

Gorham, D.A., Rickerby, D.G., 1975. A hydraulic strength test for brittle samples. Journal of physics E: Scientific Instruments 8, 794–796.

Hoshide, T., Murano, J., Kusaba, R., 1998. Effect of specimen geometry on strength in engineering ceramics. Engineering Fracture Mechanics 59, 655–665.

Jayatilaka, A., 1979. Fracture of Engineering Brittle Materials. Applied Science Publishers Ltd, London.

Kassir, M.K., Sih, G.C., 1966. Three-dimensional stress distribution around an elliptical crack under arbitrary loadings. Transactions of the ASME, Series E 89, 601–611.

Kirstein, A.F., Pell, W.H., Woolley, R.M., Davis, L.J., 1966. Deflection of centrally loaded tin circular elastic plates on equally spaced point supports. Journal of Research of the National Bureau of Standards 70C, 227–244.

Kirstein, A.F., Woolley, R.M., 1967. Symmetrical bending of thin circular elastic plates on equally spaced point supports. Journal of Research of the National Bureau of Standards 71C, 1–10.

Newman Jr., C., Raju, I.S., 1981. An empirical stress intensity factor equation for the surface crack. Engineering Fracture Mechanics 15, 185–192.

Palaniswamy, A., Knauss, W.G., 1978. On the problem of crack extension in brittle solids under general loading. Mechanics Today 4, 87–148.

Selçuk, A., Atkinson, A., 2000. Strength and toughness of tape-cast yttria-stabilized zirconia. Journal of the American Ceramic Society 83, 2029–2035.

Shetty, D.K., Rosenfield, A.R., McGuire, P., Bansal, G.K., Duckworth, W.H., 1980. Biaxial flexure tests for ceramics. American Ceramic Society Bulletin 59 (12), 1193–1197.

Shetty, D.K., Rosenfield, A.R., Duckworth, W.H., Held, P.R., 1983. A Biaxial-flexure test for evaluating ceramic strengths. Journal of the American Ceramic Society 66 (1), 36–42.

Shetty, D.K., 1987. Mixed-mode fracture criteria for reliability analysis and design with structural ceramics. Journal of Engineering for Gas Turbines and Power 109, 282–289.

Sih, G.C., 1974. Strain–energy–density factor applied to mixed mode crack problems. International Journal of Fracture 10, 305–321.

Sih, G.C., Barthelemy, B.M., 1980. Mixed mode fatigue crack growth predictions. Engineering Fracture Mechanics 13, 439–451.

Sih, G.C., 1984. Handbook of Stress–Intensity Factors. Lehigh University, Bethlehem, PA, p. 31.

Singh, D., Shetty, D.K., 1989a. Facture toughness of polycrystalline ceramics in combined mode I and mode II loading. Journal of the American Ceramic Society 72, 78–84.

Singh, D., Shetty, D.K., 1989b. Microstructure effects on toughness of polycrystalline ceramics in combined mode I and mode II loading. Journal of Engineering for Gas Turbines and Power 111, 174–180.

Smith, F.W., Sorensen, D.R., 1975. Mixed-mode stress intensity factors for semi-elliptical surface cracks. Rept. No. NASA-CR-134684, NASA Lewis Research Center, Cleveland, OH.

Wachtman, J.B., 1996. Mechanical Properties of Ceramics. John Wiley, New York.

Wachtman Jr., J.B., Capps, W., Mandel, J., 1972. Biaxial flexure tests of ceramic substrates. Journal of Materials 7, 188–194.

With, G., Wagemans, H.H.M., 1989. Ball-on-ring test revisited. Journal of the American Ceramic Society 72 (8), 1538–1541.